Comparative Medicine
Copyright 2018
by the American Association for Laboratory Animal Science

Vol 68, No 1
February 2018
Pages 15–24

Original Research

Strain-specific Differences in the Effects of Lymphocytes on the Development of Insulin Resistance and Obesity in Mice

Elisavet Kodela,[1,2] Maria Moysidou,[1,2] Sevasti Karaliota,[1] Yassemi Koutmani,[1] Panagiotis Tsakanikas,[1] Konstantia Kodella,[1] Eleni A Karavia,[4] Kyriakos E Kypreos,[4] Nikolaos Kostomitsopoulos,[1,*] and Katia P Karalis[1,3]

Obesity is characterized as a chronic, low-grade inflammatory disease owing to the infiltration of the adipose tissue by macrophages. Although the role of macrophages in this process is well established, the role of lymphocytes in the development of obesity and metabolism remains less well defined. In the current study, we fed WT and *Rag1*$^{-/-}$ male mice, of C57BL/6J and BALB/c backgrounds, high-fat diet (HFD) or normal diet for 15 wk. Compared with WT mice, *Rag1*$^{-/-}$ mice of either of the examined strains were found less prone to insulin resistance after HFD, had higher metabolic rates, and used lipids more efficiently, as shown by the increased expression of genes related to fatty acid oxidation in epididymal white adipose tissue. Furthermore, *Rag1*$^{-/-}$ mice had increased Ucp1 protein expression and associated phenotypic characteristics indicative of beige adipose tissue in subcutaneous white adipose tissue and increased Ucp1 expression in brown adipose tissue. As with inflammatory and other physiologic responses previously reported, the responses of mice to HFD show strain-specific differences, with increased susceptibility of C57BL/6J as compared with BALB/c strain. Our findings unmask a crucial role for lymphocytes in the development of obesity and insulin resistance, in that lymphocytes inhibit efficient dissipation of energy by adipose tissue. These strain-associated differences highlight important metabolic factors that should be accommodated in disease modeling and drug testing.

Abbreviations: BAT, brown adipose tissue; epiWAT, epididymal WAT; HFD, high-fat diet; ITT, insulin tolerance testing; ND, normal diet; *Rag1*$^{-/-}$, recombination-activating gene 1 knockout; scWAT, subcutaneous WAT; WAT, white adipose tissue; UCP1, uncoupling protein 1

Obesity has been evolved to an epidemic with its incidence among adults and children rising globally. Several of the leading causes of death in developed countries, such as cardiovascular diseases and cancer are included in the comorbidities of obesity and the associated development of insulin resistance.[31,32] Numerous studies have demonstrated that obesity is a chronic, low-grade, inflammatory disease.[14,23] It has been well established that the hypertrophic white adipose tissue (WAT) activates the resident immune cells to secrete chemokines that promote the infiltration of WAT by a plethora of circulating immune cells such as macrophages, dendritic cells, mast cells, neutrophils, eosinophils and type 2 innate lymphoid cells.[20,22,25,36,37,43] Recent evidence implicates the cells of the adaptive immune system, particularly $CD8^+$, $CD4^+$ T cells and regulatory T cells, in the pathogenesis of obesity-associated inflammation and insulin resistance.[4,10,30,41,42] However, the exact contribution of lymphocytes in the cascade of events leading to dysregulation of energy utilization in obesity remains to be elucidated.[1,21,41] Emerging evidence demonstrates the critical role of the interaction between the immune system and metabolism in disease development,[1,30,41] making the characterization of the metabolic activity of the different mouse strains used in research imperative for the successful interpretation and translation of preclinical findings to human studies.

In this study, we investigated the role of lymphocyte deficiency in the strain-specific development of obesity. For this reason, we compared BALB/c mice, one of the most commonly used strains for immunology and inflammation- related studies, and C57BL/6J mice, the most widely used mouse strain in disease modeling, strains. Furthermore, to assess the role of lymphocytes in obesity, we used male WT mice and a line that lacks mature B and T lymphocytes, *Rag1*$^{-/-}$ mice,[26] from both strains in a standard experimental manipulation for inducing body weight gain, adipose tissue expansion, and the development of insulin resistance due to the administration of high-fat diet (HFD, 45% kcal fat) for 4 mo. Similar to the well-described immune response,[33] metabolic activity shows considerable strain-dependent variability, which most likely underlies the discrepancies among the results of similarly designed studies,[1,27,40] that has not been addressed yet to our knowledge. Our findings show that the C57BL/6J strain is prone to diet-induced obesity and insulin resistance, whereas BALB/c mice[27] are affected much less, thus demonstrating another strain-specific difference in physiologic responses, which

Received: 04 May 2017. Revision requested: 06 Jun 2017. Accepted: 02 Aug 2017.
[1]Biomedical Research Foundation of the Academy of Athens, Clinical Experimental Surgery & Translational Research, Athens, Greece;[2]University of Crete, School of Medicine, Heraklion, Crete, Greece;[3]Endocrine Division, Boston Children's Hospital, Boston, Massachuttes;[4]Department of Pharmacology, University of Patras Medical School, Patras, Greece.
[*]Corresponding author. Email: nkostom@bioacademy.gr

are important to consider in preclinical studies and drug development.

Materials and Methods

The study was performed in the laboratory animal facility of the Biomedical Research Foundation of the Academy of Athens (Athens, Greece). The facility is registered as a 'breeding' and 'user' establishment according to the Greek Presidential Decree 56/2013, which harmonizes Greek national legislation on animal experimentation with the European Community Directive 2010/63 on the Protection of Animals Used for Experimental and Other Scientific Purposes.

Animals. Male mice of *Rag1*$^{-/-}$ genotype on a C57BL/6 or BALB/c background were purchased from Jackson Laboratories (Bar Harbor, ME). WT C57BL/6J and BALB/c mice were provided by the animal facilities at the Biomedical Research Foundation of the Academy of Athens. Mice were allocated randomly into experimental groups for each genotype. All animals were group-housed in IVC (1284L, Blue Line Sealsafe, Tecniplast, Buguggiate, Italy) in the same animal room, which was supplied with HEPA-filtered air at 15 air-changes hourly at a temperature of 22 ± 2 °C, relative humidity of 55% ± 10%, a 12:12-h light:dark cycle (lights on, 0700), light intensity of 300 lx at 1 m above the floor in the middle of the room, and positive air pressure of 0.6 Pa within the room. Room conditions were monitored continuously through the central Building Management System of the animal facility. The mice had unrestricted access to water and either HFD, consisting of 45% of calories from fat (D12451, Research Diets, New Brunswick, NJ), or normal diet (ND; 4RF21, Mucedola, Milan, Italy) for 15 or 16 wk, respectively. All mice in the animal facility were screened regularly by using a health-monitoring program, in accordance to the Federation of European Laboratory Animal Science Association and were free from a wide range of pathogens.[9] At the end of the experiment, mice were euthanized by cervical dislocation. All experimental procedures reported here were approved by the competent veterinary authority of the Prefectures of Athens in accordance with the National Registration (Presidential Decree 56/2013) in harmonization to the European Directive 63/2010.

Histologic analysis. Tissues were dissected and fixed in 4% paraformaldehyde and processed for routine paraffin histology. Paraffin-embedded tissues were sectioned at 5 µm and stained with hematoxylin and eosin, according to standard protocol. Adipocyte cell size was measured by using automated MatLab-based software developed in our lab. For immunohistochemistry, the tissues were incubated with 0.1% w/v Pronase (Sigma-Aldrich, St Louis, MO) at 37 °C for 8 min, washed, and blocked with PBS containing 10% normal goat serum and 0.1% Triton X-100 (Sigma-Aldrich), followed by overnight incubation at 4 °C with the primary antibodies. UCP1 was detected by using rabbit antiUCP1 antibody (dilution, 1:500; ab10983, Abcam, Cambridge, United Kingdom). After several washes with PBS, the tissue was incubated for 2 h with the secondary antibody, AlexaFluor 488-labeled donkey antirabbit IgG (Thermo Fisher Scientific, Braintree, MA). Another washing step was followed by incubation in 4,6-diamidin-2-phenylindol and further washes before the sections were mounted by using Vectashield mounting medium (Vector Labs, Burlingame, CA).

Indirect calorimetry. Metabolic measurement was performed by using an indirect calorimetry system (Oxymax, Columbus Instruments, Columbus, OH). In short, mice were singly housed for 2 d for acclimation, weighed, and then housed individually in specifically designed calorimeter chambers with unrestricted access to diet and water for 72 h under a 12:12-h light:dark cycle and ambient temperature of 22 °C. Metabolic parameters (VO_2, VCO_2, and rates) were determined at system settings of an air flow of 0.6 L/min and sample flow rate of 0.5 L/min. The system was calibrated against a standard gas mixture to measure O_2 consumed (that is, VO_2, mL/kg/h) and CO_2 generated (VCO_2, mL/kg/h). Metabolic rate, respiratory quotient (ratio of VCO_2/VO_2, RER), and activity (counts) were evaluated over a 48-h period.

Quantitative real-time RT-PCR analysis. Total RNA was isolated from tissues by using TRI reagent (Sigma–Aldrich) and was treated with DNase (DNA-free kit, Ambion, Austin, TX). cDNA was made from 2 µg total RNA by using MMLV reverse transcriptase (Invitrogen, Carlsbad, CA) and was initiated from random hexamer primers (Life Technologies, Waltham, MA). Quantitative real-time PCR analysis was performed using RT^2 SYBR Green qPCR Master Mix (SA Biosciences, Frederick, MD) in a Prism 7000 Sequence Detection System (Applied Biosystems, Carlsbad, CA). Primers used for real-time PCR analysis were: actin (forward, 5′ CCC AGG CAT TGC TGA CAG G 3′; reverse, 5′ TGG AAG GTG GAC AGT GAG GC 3′); Pgc1α (forward, 5′ TCA CCC TCT GGC CTG ACA AAT CTT 3′; reverse, 5′ TTT GAT GGG CTA CCC ACA GTG TCT 3′); Lipe (forward, 5′ AAG GAC TTG AGC AAC TCA GA 3′; reverse, 5′ TTG ACT ATG GCT GAC GTG TA 3′); Ucp1 (forward, 5′ TCT TCT CAG CCG GAG TTT CAG CTT 3′; reverse, 5′ ACC TTG GAT CTG AAG GCG GAC TTT 3′); Cidea (forward, 5′ ATC ACA ACT GGC CTG GTT ACG 3′; reverse, 5′ TACTACCCGGTGTCCATTTCT 3′); Prdm16 (forward, 5′ CAG CAC GGT GAA GCC ATT C 3′; reverse, 5′ GCG TGC ATC CGC TTG TG 3′); Dgat (forward, 5′ TCA TGG GTG TCT GTG GGT TA 3′; reverse, 5′ CAG AGT GAA ACC AGC CAA CA 3′); Cpt1α (forward, 5′ GTC AAG CCA GAC GAA GAA CA 3′; reverse, 5′ CGA GAA GAC CTT GAC CAT AG 3′); Adipoq (forward, 5′ GGA GAT GCA GGT CTT CTT G 3′; reverse, 5′ TTC TCC AGG CTC TCC TTT 3′); Tnfα (forward, 5′ TCT CAT GCA CCA CCA TCA AGG ACT 3′; reverse, 5′ ACC ACT CTC CCT TTG CAG AAC TCA 3′), iNOS (forward, 5′ CAG AGG ACC CAG AGA CAA GC 3′; reverse, 5′ CCT GGC CAG ATG TTC CTC TA 3′); and IL6 (forward, 5′ TCC AGT TGC CTT CTT GGG ACT GA 3′; reverse, 5′ TAA GCC TCC GAC TTG TGA AGT GGT 3′). Gene expression levels were normalized to actin and calculated according to the $2^{-\Delta\Delta Ct}$ method.

Glucose tolerance testing. For glucose tolerance testing, mice were fasted overnight. The next morning, glucose levels in tail blood were measured by using a standard glucometer (Contour XT, Bayer, IN) before and at timed intervals (0, 15, 30, 60 and 120 min) after intraperitoneal injection of D-glucose (2 g/kg; Gibco, Grand Island, NY).

Insulin tolerance testing. After a 5-h fast, mice were injected with insulin (1U/kg IP; Sanofi Aventis, Somerset, NJ). Glucose concentrations in blood collected from the tail vein at 0, 15, 30, 60 and 120 min after insulin injection were measured by using a handheld glucometer (Contour XT, Bayer, IN).

Measurement of plasma total cholesterol and triglyceride contents. Mice were fasted for 16 h, after which the cholesterol and triglyceride contents in serum collected from all mice were measured as described previously.[15]

Statistical Analysis. Data are presented as mean ± SEM. Differences were analyzed by using unpaired 2-tailed *t* tests (for single comparisons) or 2-way ANOVA with repeated measures followed by post hoc Bonferroni multiple-comparison tests by using Prism (version 5.00, GraphPad Software, La Jolla, CA). A *P* value less than 0.05 was considered significant.

Results

Effect of lymphocyte deficiency on HFD-induced adiposity. Age-matched C57BL/6J WT and *Rag1*$^{-/-}$ male mice were

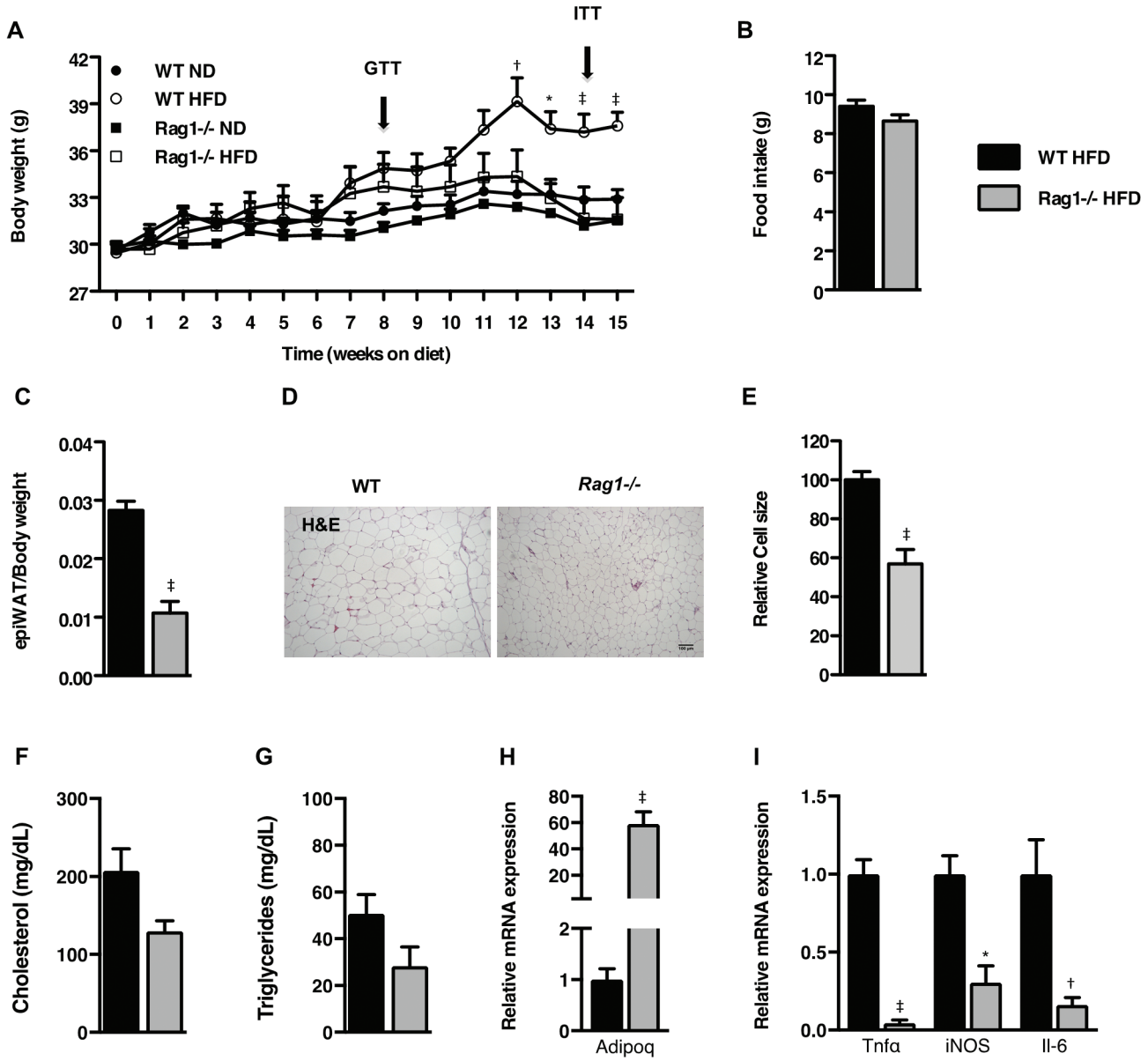

Figure 1. Effects of lymphocyte deficiency on HFD-induced obesity. (A) Body weights of WT and *Rag1*$^{-/-}$ mice fed ND or HFD for 15 wk. (B) Food intake as measured by indirect calorimetry over 72 h. (C) Epididymal fat pad weight adjusted to body weight of WT and *Rag1*$^{-/-}$ mice fed ND or HFD for 15 wk. (D) Representative histology (hematoxylin and eosin stain; scale bar, 100 µm) and (E) relative cell size of epiWAT of WT and *Rag1*$^{-/-}$ male mice fed HFD. Circulating levels of (F) fasting cholesterol and (G) triglycerides. (H) Expression of *Adipoq* gene in epiWAT. (I) Expression of inflammatory cytokine genes in the epiWAT. Data were analyzed by repeated-measures ANOVA and posthoc multiple comparison tests or *t* tests. Data are expressed as mean ± SEM; *, $P < 0.05$; †, $P < 0.01$; ‡, $P < 0.001$; $n = 3$ to 5 mice per group.

maintained on HFD for 15 wk. The patterns of the body weight gain were indistinguishable between the 2 genotypes during the first 6 wk of HFD feeding (Figure 1 A) but began to lag thereafter in the *Rag1*$^{-/-}$ mice despite their similar food intake (Figure 1 B) as measured by indirect calorimetry. The differences in body weight between the 2 genotypes became significant ($P < 0.001$) after 3 mo of HFD (Figure 1 A). The weight gain of the respective (control) groups on ND was comparable between the 2 genotypes throughout the study (Figure 1 A). As suggested by the differences in body weight, the ratio of epididymal WAT (epiWAT) to body weight was lower ($P < 0.001$) in the *Rag1*$^{-/-}$ mice as compared with their WT counterparts at the end of the experiment (Figure 1 C). The decreased mass of the epiWAT depot together with the smaller adipocyte size in *Rag1*$^{-/-}$ mice ($P < 0.001$; Figure 1 D and E) indicate compromised energy storage in the WAT. This result might be due to more efficient utilization of excess energy, unmasked by the hypercaloric diet (Figure 1 C through E). In line with this hypothesis, fasting cholesterol and triglyceride levels in the circulation showed a trend toward lower values in *Rag1*$^{-/-}$ mice ($P = 0.08$ and $P = 0.12$, respectively; Figure 1 F and G), whereas the adiponectin expression in their epiWAT was significantly higher ($P < 0.001$) than in WT controls (Figure 1 H). As expected, the expression of inflammatory cytokines was significantly lower ($P < 0.05$) in the epiWAT of *Rag1*$^{-/-}$ mice than in WT controls (Figure 1 I), in further support of the protective *Rag1*$^{-/-}$ phenotype against the development of HFD-induced obesity and associated endpoints.

Effects of lymphocyte deficiency on insulin sensitivity. To assess insulin sensitivity, we conducted glucose tolerance testing at experimental week 8. Whereas C57BL/6J WT mice exhibited

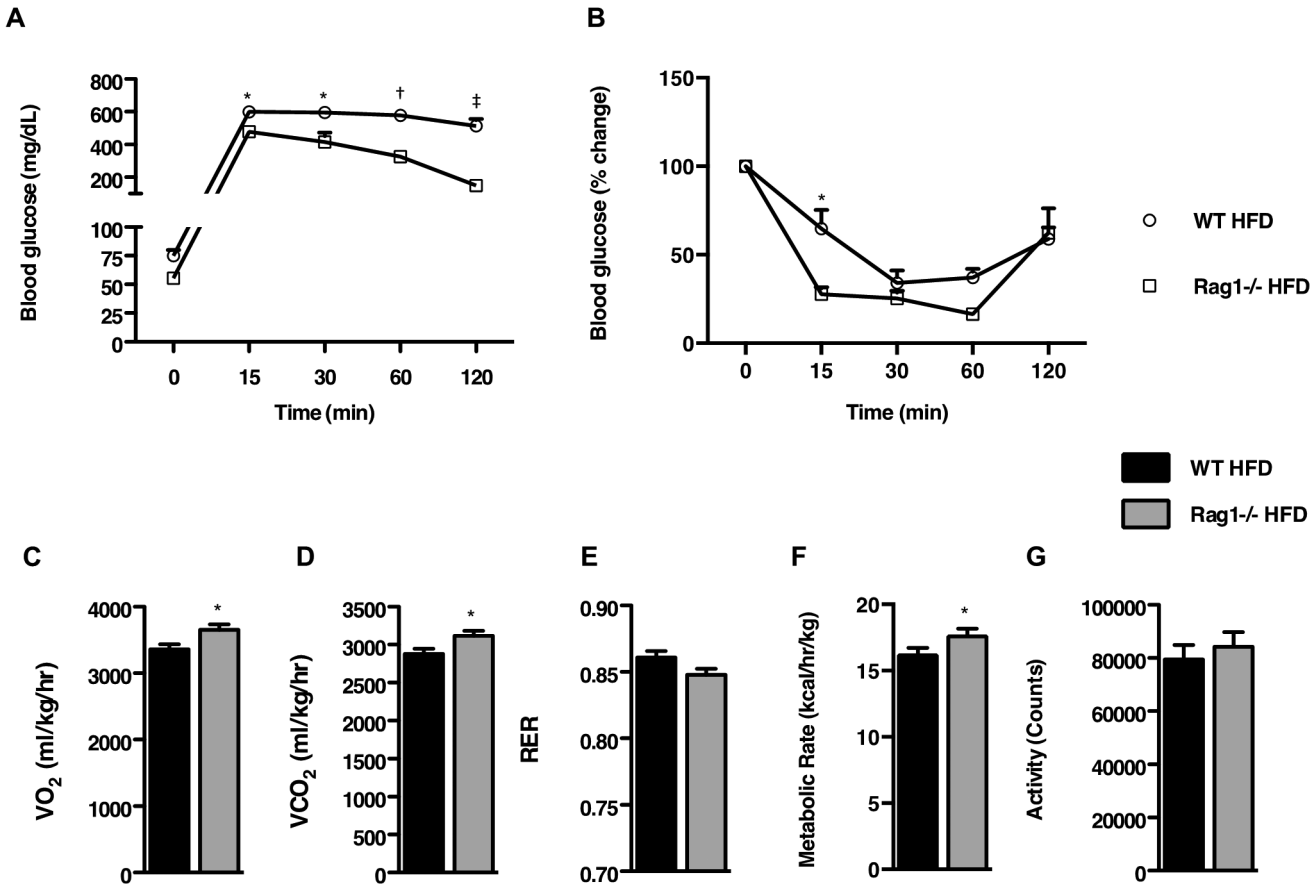

Figure 2. Effects of lymphocyte deficiency on insulin sensitivity and metabolic parameters. (A) Glucose tolerance test of WT and *Rag1*$^{-/-}$ mice fed a ND or HFD for 8 wk. (B) Insulin tolerance test of WT and *Rag1*$^{-/-}$ mice fed a ND or HFD for 14 wk. Data were analyzed by repeated measures ANOVA and posthoc multiple comparison tests. Data are expressed as mean ± SEM; *, $P < 0.05$; †, $P < 0.01$; ‡, $P < 0.001$; $n = 3$ or 4 mice per group. (C through G) Measurement of metabolic characteristics over 48 h in WT and *Rag1*$^{-/-}$ mice fed HFD. (C), VO_2. (D) VCO_2. (E) Respiratory quotient (RER). (F) Metabolic rate. (G) Total activity (G). Data were analyzed by *t* test and are expressed as mean ± SEM; *, $P < 0.05$; †, $P < 0.01$; ‡, $P < 0.001$; $n = 6$ to 8 mice per group.

elevated blood glucose levels at 2 h after glucose administration, *Rag1*$^{-/-}$ mice had much better ($P < 0.001$) tolerance to the glucose challenge (Figure 2 A). In the same manner, *Rag1*$^{-/-}$ HFD fed mice exhibited a much better ($P < 0.05$) response to insulin over the course of insulin tolerance testing (ITT) than their WT counterparts (Figure 2 B).

Metabolic activity in lymphocyte-deficient mice. Next, we used indirect calorimetry to assess differences in the metabolic phenotypes of C57BL/6J WT and *Rag1*$^{-/-}$ mice. In agreement with the earlier-described findings, *Rag1*$^{-/-}$ mice showed increased ($P < 0.05$) oxygen consumption (Figure 2 C) and carbon dioxide production (Figure 2 D) despite their similar food intake (Figure 1 B) and motor behaviors (Figure 2 G) to those of the WT mice. In addition, RER tended to be slightly lower in the *Rag1*$^{-/-}$ mice ($P = 0.08$; Figure 2 E), indicating the preferential use of fatty acids instead of carbohydrates as the primary energy source. In addition, the metabolic rate was higher ($P < 0.05$) in *Rag1*$^{-/-}$ mice than WT mice (Figure 2 F).

Effects of lymphocyte deficiency on lipid storage in WAT and dissipation of energy. To gain insight into why *Rag1*$^{-/-}$ mice on HFD are protected from the development of insulin resistance and obesity, we first assessed lipid metabolism in their various WAT depots. Gene expression profiling identified increased ($P < 0.05$) expression of genes involved in lipid oxidation and lipolysis in the *Rag1*$^{-/-}$ epiWAT depot compared with the WT tissue (Figure 3 A). Furthermore, the reduced ($P < 0.05$) expression of diglyceride acyltransferase in *Rag1*$^{-/-}$ mice (Figure 3 A) might be directly linked to their resistance to the development of obesity.

We then examined the subcutaneous WAT (scWAT) depot of the *Rag1*$^{-/-}$ mice, a fat depot that demonstrates plasticity, in that it shifts from energy storage to energy dissipation through the development of areas of 'beige fat,' which is rich in mitochondria.[5,13,44] Histologic analysis of scWAT revealed smaller adipocytes that stained strongly positive with a specific antiUCP1 antibody, in the *Rag1*$^{-/-}$ but not in the WT tissue (Figure 3 B i and ii). This staining pattern characterizes the induction of beige adipogenesis, indicative of the increased tissue content in adipocytes capable of increased energy utilization.[29,34] The upregulation ($P < 0.05$) of genes that are highly expressed in beige adipocytes, such as cell death-inducing DFFA-like effector α (*Cidea*) and peroxisome proliferator-activated receptor γ coactivator 1-α (*Pgc1a*), in *Rag1*$^{-/-}$ compared with WT scWAT (Figure 3 C) was in line with the histologic findings.

Lastly, we analyzed the BAT depot, because changes in BAT activity can profoundly affect body weight and alter glucose homeostasis.[8] As anticipated, lipid droplets were smaller ($P < 0.05$) in *Rag1*$^{-/-}$ adipocytes than in WT cells (Figure 3 D). In agreement with this phenotype, *Ucp1* expression was upregulated ($P < 0.05$) in the BAT of *Rag1*$^{-/-}$ HFD-fed mice, in line with increased thermogenic capacity, compared with that in WT controls (Figure 3 E).

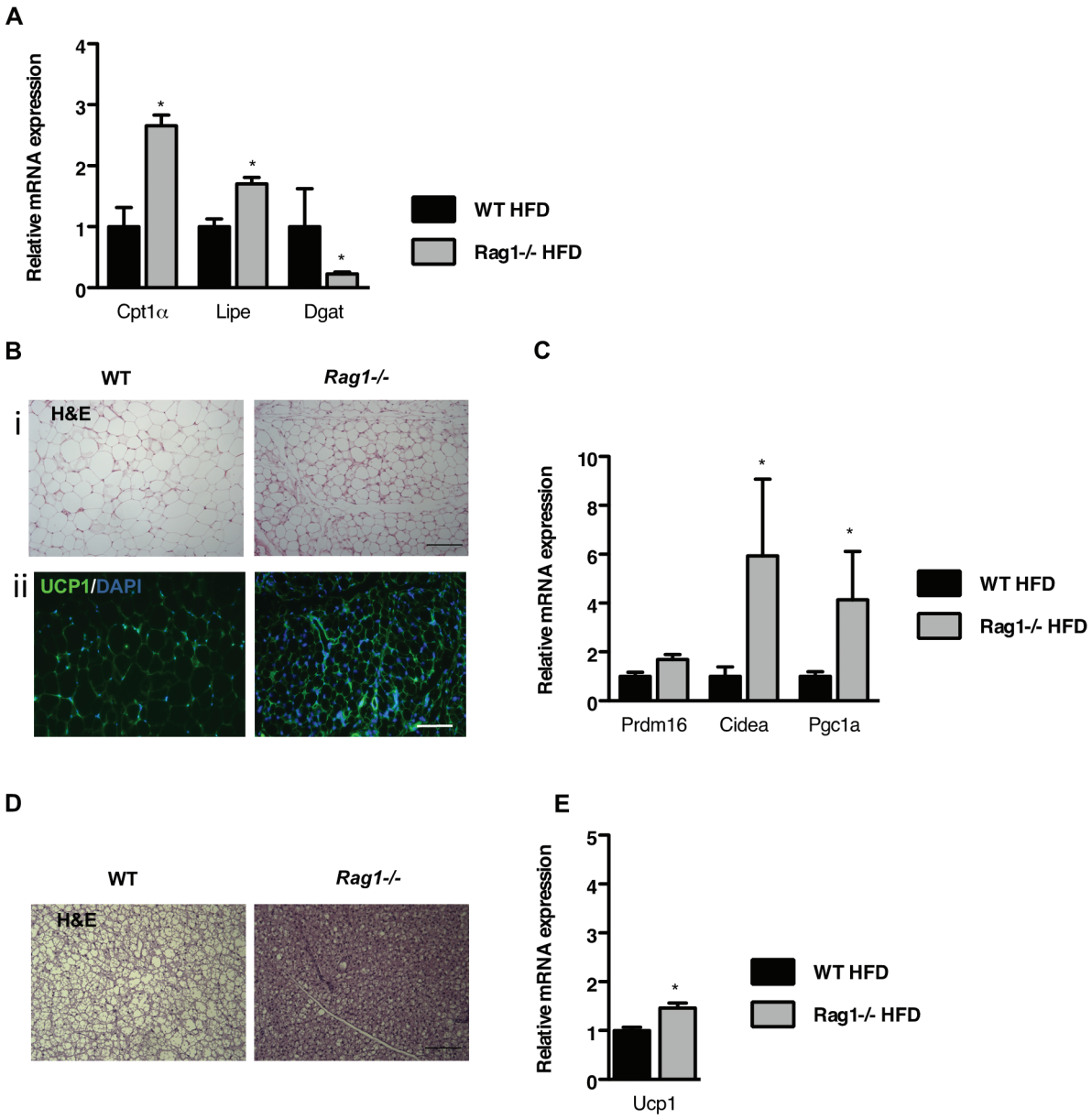

Figure 3. Lymphocyte deficiency favors the dissipation of energy in the various adipose depots. (A) Expression of genes associated with fatty acid oxidation, lipogenesis, and lipolysis in the epiWAT of WT and *Rag1*$^{-/-}$ male mice fed HFD. Data were analyzed by *t* test. (B) Representative hematoxylin and eosin (i; scale bar, 100 µm) and UCP1 staining (ii; scale bar, 50 µm) of scWAT of WT and *Rag1*$^{-/-}$ male mice fed HFD. (C) Expression of beige genes in the scWAT of WT and *Rag1*$^{-/-}$ male mice placed on HFD. (D) Representative hematoxylin and eosin staining (scale bar, 100 µm) of brown adipose tissue (BAT) in WT and *Rag1*$^{-/-}$ male mice fed HFD. (E) Expression of *Ucp1* in the BAT of WT and *Rag1*$^{-/-}$ male mice fed HFD. Data were analyzed by *t* test and are expressed as mean ± SEM; *, $P < 0.05$; $n = 3$ to 5 mice per group.

Strain-associated differences in the responses of *Rag1*$^{-/-}$ mice to HFD. As discussed earlier, *Rag1*$^{-/-}$ mice are primarily used in modeling autoimmune and specific infectious or inflammatory processes. For these purposes, the BALB/c strain is selected, due to its demonstrated sensitivity to immune challenge and its Th2-biased responses.[33] A prime example of this bias comes from studies on asthma and other allergic responses.[6,12] In addition, BALB/c mice are relatively resistant to the development of HFD-induced obesity.[27,38] Given our findings from the C57BL/6J *Rag1*$^{-/-}$ mice, we decided to compare their responses to HFD with those of BALB/c *Rag1*$^{-/-}$ mice and assess whether the previously shown differing sensitivity to immune challenges extends to their responses to HFD (Figure 4).

By the end of the experiment, WT ND mice had gained 0.1% ± 1% and *Rag1*$^{-/-}$ ND mice 4.3% ± 4.0% in body weight (Figure 4 A), whereas WT HFD mice gained 19.8% ± 3.2% and *Rag1*$^{-/-}$ HFD 12.0% ± 2.0% (Figure 4 B). The slight decrease in body weight at the end of the experiment likely is related to ITT, a stressor for all mice, performed just a few days earlier. Regarding interstrain differences in WT mice of the same genotype, body weight gain was more pronounced in C57BL/6J mice (28.0% ± 2.8% increase) than in BALB/c mice (19.8% ± 3.2%; $P < 0.05$; Figures 1 A and 4 A). Notably, circulating cholesterol ($P < 0.05$) and triglyceride levels were lower in BALB/c *Rag1*$^{-/-}$ mice (Figure 4 G and H), whereas the expression of adiponectin in epiWAT was significantly ($P < 0.01$) increased (Figure 4 I). In addition, expression of inflammatory cytokines in the epiWAT of *Rag1*$^{-/-}$ mice of the BALB/c strain was significantly ($P < 0.01$) lower than in WT controls (Figure 4 J), similar to our findings from studying C57BL/6J mice (Figures 1 I and 5).

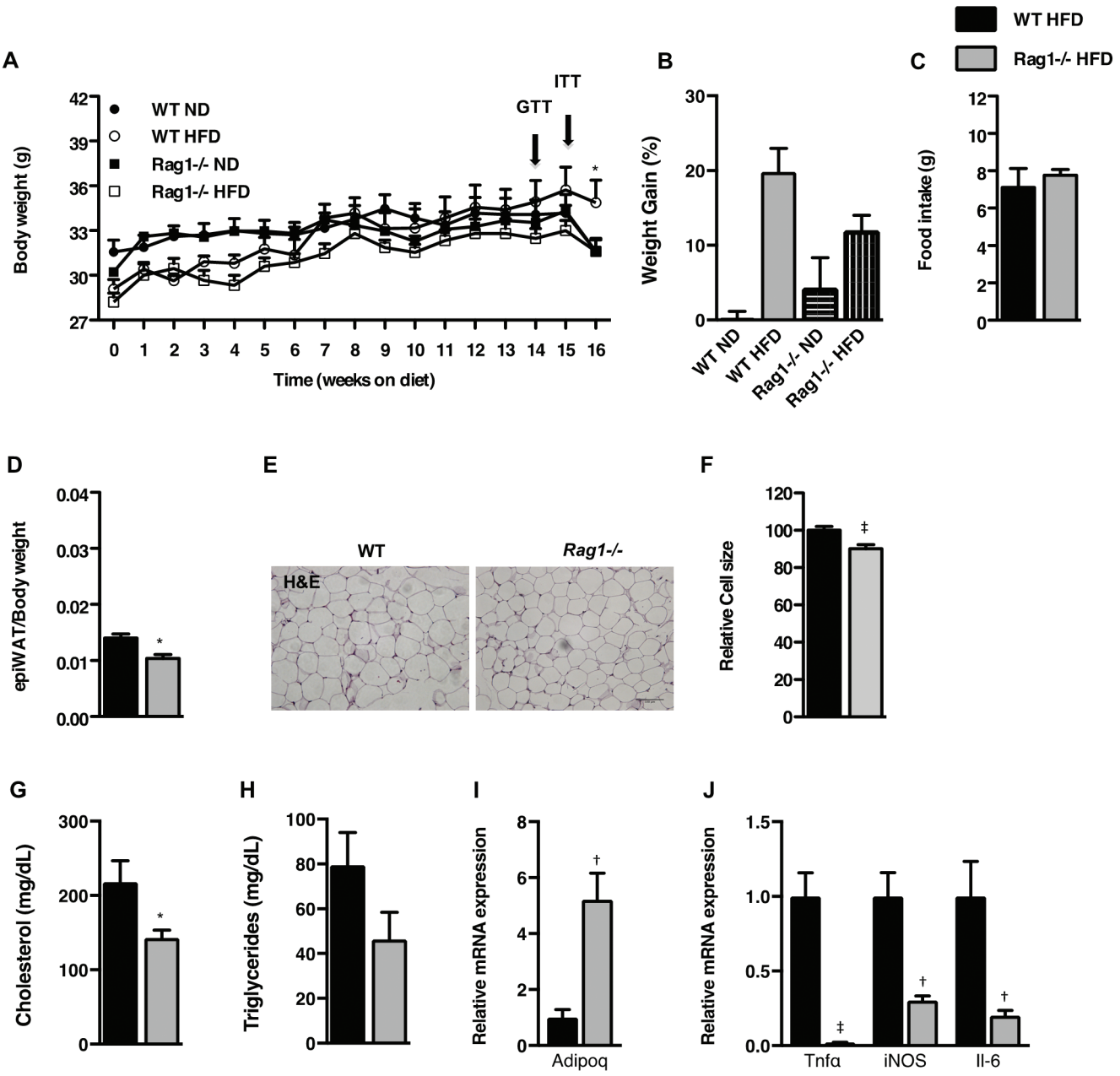

Figure 4. Effects of lymphocyte deficiency on HFD-induced obesity in the BALB/c strain. (A) Body weights of WT and *Rag1*$^{-/-}$ mice fed ND or HFD for 16 wk. (B) Body weight gain at the end of the experiment. (C) Food intake over 72 h as measured by indirect calorimetry. (D) Epididymal fat pad weight adjusted to body weight of WT and *Rag1*$^{-/-}$ mice placed on ND or HFD for 16 wk. (E) Representative hematoxylin and eosin staining (scale bar, 100 µm) and (F) relative cell size of epiWAT of WT and *Rag1*$^{-/-}$ male mice fed HFD. (G and H) Circulating levels of (G) fasting cholesterol and (H) triglycerides. (I) Expression of *Adipoq* in the epiWAT. (J) Expression of inflammatory cytokine genes in the epiWAT. Data were analyzed by repeated-measures ANOVA and posthoc multiple comparison tests or *t* test and are expressed as mean ± SEM*, $P < 0.05$; †, $P < 0.01$; ‡, $P < 0.001$; $n = 3$ to 5 mice per group.

Along these lines, BALB/c WT mice on HFD were less prone than HFD-fed C57BL/6J WT mice to developing insulin resistance, as shown by the results of glucose tolerance testing ($P < 0.01$; Figures 2 A and 5 A), and ITT ($P < 0.05$; Figures 2 B and 5 B). Similar to our findings in the C57BL/6J strain, BALB/c *Rag1*$^{-/-}$ mice were less prone to the metabolic effects of HFD, as shown by their body weight gain, adiposity, and insulin sensitivity, compared with their WT counterparts.

Regarding metabolic activity as measured by indirect calorimetry, *Rag1*$^{-/-}$ mice showed increased oxygen consumption ($P < 0.05$; Figure 5 C) and carbon dioxide production ($P < 0.05$; Figure 5 D), as compared with WT mice, despite the similar food intake (Figure 4 C) and motor behavior (Figure 5 G) in the 2 groups. Furthermore, RER did not differ between groups (Figure 5 E), despite the higher metabolic rate of the *Rag1*$^{-/-}$ mice ($P < 0.05$; Figure 5 F). These findings were similar to those in the C57BL/6J mice (Figure 2 C through G) demonstrating that genotype-related differences remain consistent between the 2 mouse strains used (Figure 6).

This response is further highlighted by the increased energy dissipation via the adipose tissue, demonstrated by the induced fatty acid oxidation in the epiWAT ($P < 0.01$; Figure 6 A) and the activation of thermogenic factors such as Ucp1 in the scWAT ($P < 0.01$; Figure 6 B and C) and BAT depots ($P < 0.01$; Figure 6 D

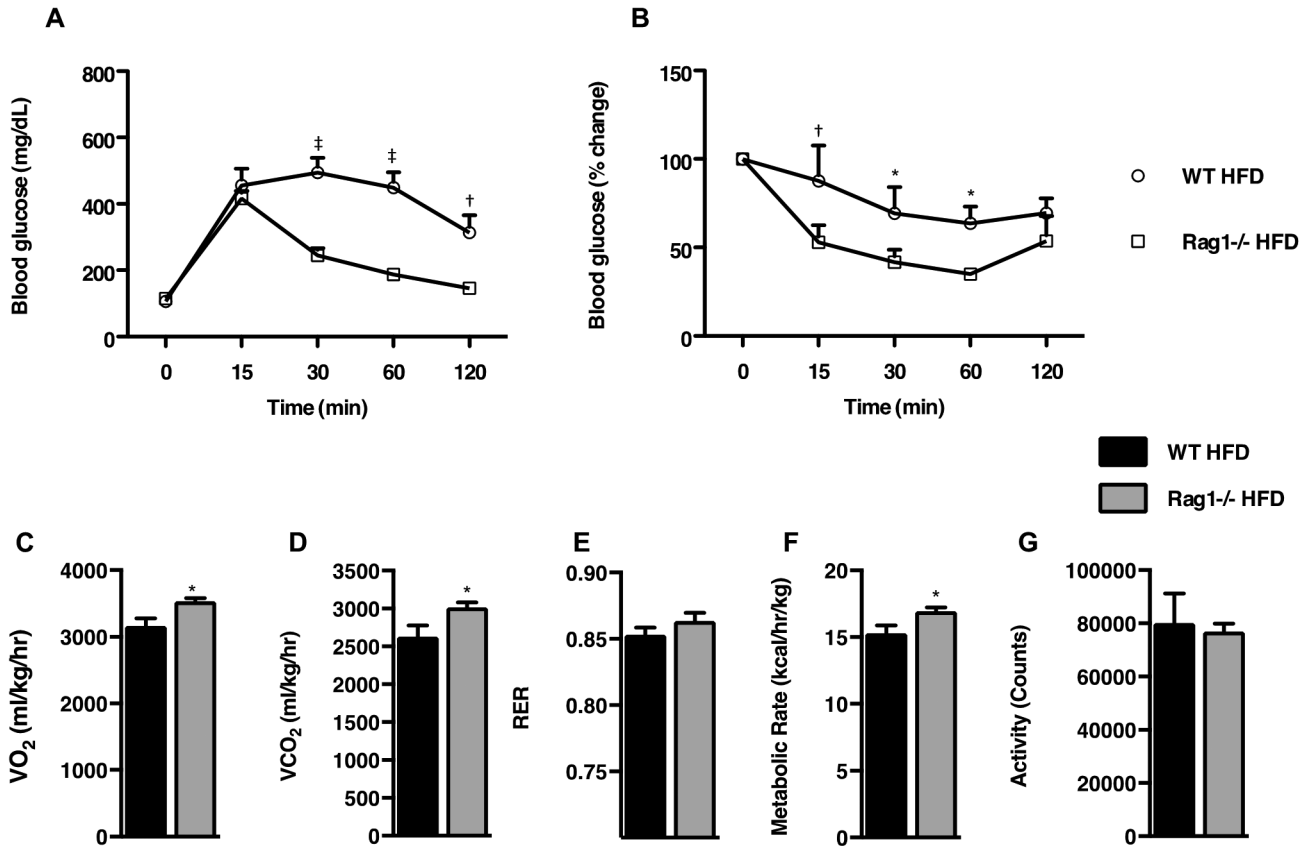

Figure 5. Effects of lymphocyte deficiency on insulin sensitivity and metabolic parameters in the BALB/c strain. (A) Glucose tolerance test of WT and *Rag1*$^{-/-}$ mice fed a ND or HFD for 14 wk. (B) Insulin tolerance test of WT and *Rag1*$^{-/-}$ mice fed a ND or HFD for 15 wk. (C through G) Measurement of metabolic characteristics over 48 h by using indirect calorimetry. (C) VO_2, (D) VCO_2, (E) RER, (F) metabolic rate, and (G) total activity in WT and *Rag1*$^{-/-}$ mice placed on HFD. Data were analyzed by repeated-measures ANOVA and posthoc multiple-comparison tests and are expressed as mean ± SEM *,$P < 0.05$; †, $P < 0.01$; ‡, $P < 0.001$; $n = 3$ to 5 mice per group.

and E) in the BALB/c *Rag1*$^{-/-}$ mice. These findings are similar to those from the C57BL/6J mice studies (Figure 3).

Discussion

In summary, the findings of our study suggest that metabolic activity is greater in *Rag1*$^{-/-}$ mice than WT mice and that this difference is maintained in 2 of the most commonly used mouse strains. As a result, *Rag1*$^{-/-}$ mice exhibit resistance to HFD-mediated changes in body weight, adiposity, and insulin sensitivity. Intrastrain differences in body weight, adiposity, and insulin resistance were identified in the current study, as has been shown with other physiologic responses, such as immune activation.[19] These data suggest that lymphocyte deficiency confers prophylaxis against HFD-induced obesity even in mice with associated activation of the innate immune system, such as *Rag1*$^{-/-}$ mice.[2,35]

In the current study, we applied the model of high-fat diet-induced obesity to assess the effects of lymphocyte deficiency on adiposity in 2 mouse strains. For this reason, we compared the metabolic responses of 2 most commonly used *Rag1*$^{-/-}$ mouse strains, C57BL/6J and BALB/c. Our findings demonstrate the importance of the adaptive immune system in the regulation of the dissipation of energy and the corresponding development of obesity and insulin resistance after a hypercaloric diet in these mouse strains. In addition, we confirmed that WT BALB/c mice are more resistant than the WT C57BL/6J mice to the diet-induced obesity, consistent with the literature.[27]

Previous studies have sought to reveal the relationship between HFD and the adaptive immune response in the development of obesity but have yielded diverse conclusions. In one study,[41] C57BL/6 *Rag1*$^{-/-}$ mice fed a 60% fat diet for 14 wk gained more body weight and were less sensitive to insulin than their WT counterparts. Using the same mouse line, other researchers who maintained C57BL/6J mice for 11 wk on a diet containing 42.2% fat showed that *Rag1*$^{-/-}$ gained more weight than WT mice, although insulin resistance did not differ between groups. In another study,[7] C57BL/6J *Rag2*$^{-/-}$ and WT mice maintained on a 45% fat diet for 12 wk had similar body weight and insulin resistance. Furthermore, compared with their WT counterparts, B6.129S7 *Rag1*$^{-/-}$ mice fed a 30% fructose solution for 12 wk gained less body weight and retained insulin sensitivity.[1] Overall, the differences among the studies cited might be due to variability between the applied diets or to differences in the genetic background or age of the mice used. Our current results were obtained from age-matched C57BL/6J and BALB/c male mice and provide strong evidence of the protective phenotype of *Rag1*$^{-/-}$ mice against HFD -induced adiposity and insulin resistance. Importantly, the characterization of both strains has confirmed their suitability for obesity studies and demonstrated that experiments with both strains are unnecessary, leading to use of reduced numbers of mice.

In this context, we have shown that, over a 15-wk period on a hypercaloric diet, *Rag1*$^{-/-}$ mice, which are unable to mount adaptive immune responses, do not gain as much weight as their WT counterparts, despite their similar food intake. The difference in body weight between the 2 genotypes was associated with decreased epiWAT mass and adipocytes of smaller size. Furthermore, the hypercaloric diet used rendered the WT

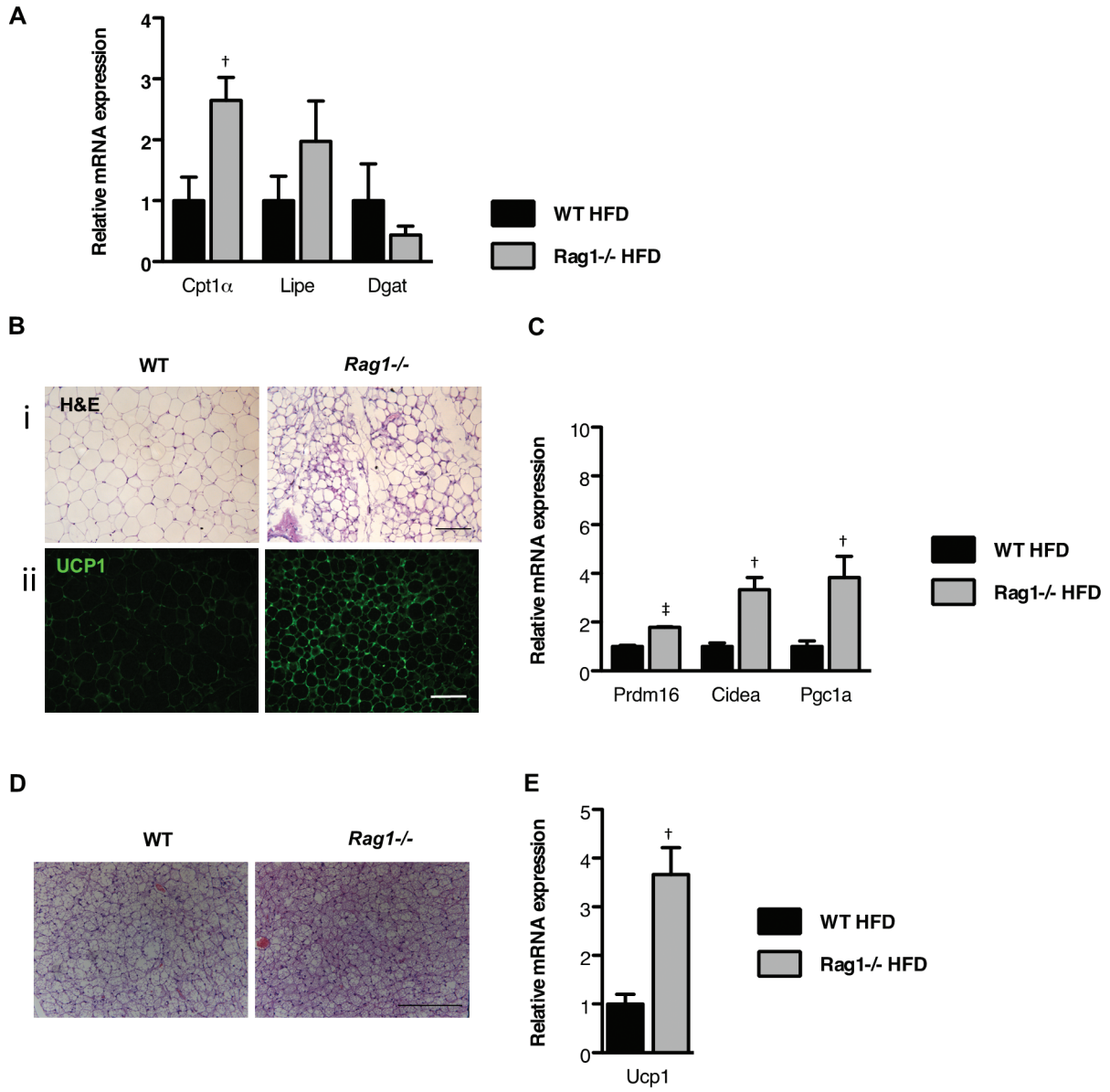

Figure 6. Lymphocyte deficiency alters lipid metabolism in WAT and favors dissipation of energy. (A) Expression of genes associated with fatty acid oxidation, lipogenesis, and lipolysis in the epiWAT of WT and *Rag1*$^{-/-}$ male mice fed HFD. (B) Representative hematoxylin and eosin staining (i; scale bar, 100 µm) and UCP1 staining (ii; scale bar, 50 µm) of scWAT of WT and *Rag1*$^{-/-}$ male mice fed HFD. (C) Expression of genes associated with beige adipose tissue in the scWAT of WT and *Rag1*$^{-/-}$ male mice fed HFD. (D) Representative hematoxylin and eosin staining (scale bar, 100 µm) of BAT of WT and *Rag1*$^{-/-}$ male mice fed HFD. (E) Production of Ucp1 in the BAT of WT and *Rag1*$^{-/-}$ male mice fed HFD. Data were analyzed by *t* test and are expressed as mean ± SEM; *, $P < 0.05$; †, $P < 0.01$; ‡, $P < 0.001$; $n = 3$ or 4 mice per group.

mice more insulin-resistant, whereas their *Rag1*$^{-/-}$ counterparts remained more sensitive as shown by the results of glucose tolerance testing and ITT. These responses are in line with the resistance of *Rag1*$^{-/-}$ mice to the development of obesity as compared with their WT counterparts. The detailed assessment of their increased metabolic rate and oxygen consumption, hallmarks of catabolic phenotypes, yielded hints regarding why animals unable to mount adaptive immune responses bear this 'protective' phenotype. This finding is in agreement with their increased expression of epiWAT *Cpt1α*, an early gene in the mitochondrial fatty acid oxidation cascade.[28] In addition, we identified more abundant UCP1 production, a protein that indicates increased thermogenic capacity, in the scWAT of the *Rag1*$^{-/-}$ mice; this finding is in line with their metabolic phenotype. Furthermore, the increased expression of *Cidea* and *Pgc1a*, characteristic of beige adipose tissue and mitochondrial biogenesis, respectively, in the *Rag1*$^{-/-}$ scWAT provides evidence for activated energy dissipation mechanism also in line with overall protection from HFD-induced obesity. Finally, the *Rag1*$^{-/-}$ BAT showed increased *Ucp1* expression and decreased lipid droplet size, compared with the WT BAT.

According to our data, *Rag1*$^{-/-}$ mice are less prone to develop obesity, despite their more activated innate immune system; most likely this is an adaptive response for the lack of a functional adaptive immune system.[19] In particular, we found that after 15 to 16 wk of feeding the HFD, the expression of proinflammatory cytokines in the epiWAT was significantly lower in the *Rag1*$^{-/-}$ mice compared with the WT. This result is consistent with the protected phenotype of *Rag1*$^{-/-}$ mice, which are able to metabolize the increased lipids provided via the diet and increase their energy expenditure; in contrast, in WT mice, the increased lipids are stored in the expanding adipose

tissue, resulting in lipotoxic effects. One of the hallmarks of the expanding adipose tissue in obesity is its infiltration by macrophages.[39,45] This macrocytic infiltration likely is orchestrated by $CD8^+$ T cells, given that their numbers in the adipose tissue increase before macrophage infiltration occurs;[30] consequently a futile cycle is established, leading to increased adiposity and inflammation. This process indicates how lymphocytes are critical for macrophage activation in the expanded adipose tissue—an observation in agreement with the compromised response of the *Rag1*$^{-/-}$ mice to obesity and insulin resistance over time. Together, these findings suggest that the contribution of the adaptive immune system in the induction of adiposity may be primarily due to altered lipid utilization within the various adipose tissue depots.[1,7,21,41]

Emerging evidence suggests 'beige-ing' of scWAT as a potential therapeutic target for obesity and insulin resistance. Several either gain- or loss-of-function mouse models for genes involved in the development and activity of beige adipose tissue are resistant to weight gain.[13] Recently, molecules such as IRISIN and FGF21, which induce beige adipose tissue, are considered as promising targets for the treatment of human obesity.[3,11] Further support on the therapeutic potential of beige adipocytes, is provided by studies showing that the implantation of human beige adipocytes in the scWAT of obese NOD-scid IL2rg^{null} mice improved glucose tolerance.[24] Our findings suggest the possibility that lymphocytes act as a brake for beige adipogenesis, either directly or through their effects on innate immune cells.

In summary, our results provide strong evidence of the effects of lymphocyte deficiency on the dissipation of energy and the induction of beige adipogenesis in mice, independent of the strain studied. Given the number of studies that involve lymphocyte-deficient mouse models, consideration of the associated differences in metabolic activity may provide useful insights for interpretation of findings and even for more informative experimental designs. Finally, these findings may contribute to the design of new therapeutic approaches, including immunomodulatory interventions,[16,17] for states of altered lymphocyte numbers, including not only obesity but also severe wasting, a serious unmet medical need associated with chronic devastating conditions including cancer, infectious disease, heart failure, Alzheimer disease, and more.[18]

Acknowledgments

This work was supported by Greek national funds through the Operational Program "Education and Lifelong Learning of the National Strategic Reference Framework (NSRF)-Research Funding Program: Herakletus II and NSRF 2007–2013 Programme for Development (EU Regional Development Fund)," Greek Ministry of Education and Religious Affairs, Culture, and Sports.

References

1. **Bhattacharjee J, Kumar JM, Arindkar S, Das B, Pramod U, Juyal RC, Majumdar SS, Nagarajan P.** 2014. Role of immunodeficient animal models in the development of fructose-induced NAFLD. J Nutr Biochem **25:**219–226.
2. **Bombeiro AL, Santini JC, Thome R, Ferreira ER, Nunes SL, Moreira BM, Bonet IJ, Sartori CR, Verinaud L, Oliveira AL.** 2016. Enhanced immune response in immunodeficient mice improves peripheral nerve regeneration following axotomy. Front Cell Neurosci **10:**1–14.
3. **Boström P, Wu J, Jedrychowski MP, Korde A, Ye L, Lo JC, Rasbach KA, Bostrom EA, Choi JH, Long JZ, Kajimura S, Zingaretti MC, Vind BF, Tu H, Cinti S, Hojlund K, Gygi SP, Spiegelman BM.** 2012. A PGC1α-dependent myokine that drives brown-fat-like development of white fat and thermogenesis. Nature **481:**463–468.
4. **Cipolletta D, Feuerer M, Li A, Kamei N, Lee J, Shoelson SE, Benoist C, Mathis D.** 2012. PPARγ is a major driver of the accumulation and phenotype of adipose tissue T_{reg} cells. Nature **486:**549–553.
5. **Cohen P, Levy JD, Zhang Y, Frontini A, Kolodin DP, Svensson KJ, Lo JC, Zeng X, Ye L, Khandekar MJ, Wu J, Gunawardana SC, Banks AS, Camporez JP, Jurczak MJ, Kajimura S, Piston DW, Mathis D, Cinti S, Shulman GI, Seale P, Spiegelman BM.** 2014. Ablation of PRDM16 and beige adipose causes metabolic dysfunction and a subcutaneous to visceral fat switch. Cell **156:**304–316.
6. **De Vooght V, Vanoirbeek JA, Luyts K, Haenen S, Nemery B, Hoet PH.** 2010. Choice of mouse strain influences the outcome in a mouse model of chemical-induced asthma. PLoS One **5:**1–9.
7. **Duffaut C, Galitzky J, Lafontan M, Bouloumie A.** 2009. Unexpected trafficking of immune cells within the adipose tissue during the onset of obesity. Biochem Biophys Res Commun **384:**482–485.
8. **Feldmann HM, Golozoubova V, Cannon B, Nedergaard J.** 2009. UCP1 ablation induces obesity and abolishes diet-induced thermogenesis in mice exempt from thermal stress by living at thermoneutrality. Cell Metab **9:**203–209.
9. **FELASA working group on revision of guidelines for health monitoring of rodents and rabbits, Mahler Convenor M, Berard M, Feinstein R, Gallagher A, Illgen-Wilcke B, Pritchett-Corning K, Raspa M.** 2014. FELASA recommendations for the health monitoring of mouse, rat, hamster, guinea pig, and rabbit colonies in breeding and experimental units. Lab Anim **48:**178–192. PubMed
10. **Feuerer M, Herrero L, Cipolletta D, Naaz A, Wong J, Nayer A, Lee J, Goldfine AB, Benoist C, Shoelson S, Mathis D.** 2009. Lean, but not obese, fat is enriched for a unique population of regulatory T cells that affect metabolic parameters. Nat Med **15:**930–939.
11. **Fisher FM, Kleiner S, Douris N, Fox EC, Mepani RJ, Verdeguer F, Wu J, Kharitonenkov A, Flier JS, Maratos-Flier E, Spiegelman BM.** 2012. FGF21 regulates PGC1α and browning of white adipose tissues in adaptive thermogenesis. Genes Dev **26:**271–281.
12. **Grünig G, Warnock M, Wakil AE, Venkayya R, Brombacher F, Rennick DM, Sheppard D, Mohrs M, Donaldson DD, Locksley RM, Corry DB.** 1998. Requirement for IL-13 independently of IL-4 in experimental asthma. Science **282:**2261–2263.
13. **Harms M, Seale P.** 2013. Brown and beige fat: development, function, and therapeutic potential. Nat Med **19:**1252–1263.
14. **Hotamisligil GS, Shargill NS, Spiegelman BM.** 1993. Adipose expression of tumor necrosis factor α: direct role in obesity-linked insulin resistance. Science **259:**87–91.
15. **Karavia EA, Papachristou DJ, Liopeta K, Triantaphyllidou IE, Dimitrakopoulos O, Kypreos KE.** 2012. Apolipoprotein A-I modulates processes associated with diet-induced nonalcoholic fatty liver disease in mice. Mol Med **18:**901–912.
16. **Kavanaugh A.** 1999. An overview of immunomodulatory intervention in rheumatoid arthritis. Drugs Today (Barc) **35:**275–286.
17. **Khalil DN, Smith EL, Brentjens RJ, Wolchok JD.** 2016. The future of cancer treatment: immunomodulation, CARs, and combination immunotherapy. Nat Rev Clin Oncol **13:**273–290.
18. **Kir S, Komaba H, Garcia AP, Economopoulos KP, Liu W, Lanske B, Hodin RA, Spiegelman BM.** 2016. PTH–PTHrP receptor mediates cachexia in models of kidney failure and cancer. Cell Metab **23:**315–323.
19. **Lee YS, Li P, Huh JY, Hwang IJ, Lu M, Kim JI, Ham M, Talukdar S, Chen A, Lu WJ, Bandyopadhyay GK, Schwendener R, Olefsky J, Kim JB.** 2011. Inflammation is necessary for long-term but not short-term high-fat diet-induced insulin resistance. Diabetes **60:**2474–2483.
20. **Liu J, Divoux A, Sun J, Zhang J, Clement K, Glickman JN, Sukhova GK, Wolters PJ, Du J, Gorgun CZ, Doria A, Libby P, Blumberg RS, Kahn BB, Hotamisligil GS, Shi GP.** 2009. Genetic deficiency and pharmacological stabilization of mast cells reduce diet-induced obesity and diabetes in mice. Nat Med **15:**940–945.
21. **Liu X, Huh JY, Gong H, Chamberland JP, Brinkoetter MT, Hamnvik OP, Mantzoros CS.** 2015. Lack of mature lymphocytes results in obese but metabolically healthy mice when fed a high-fat diet. Int J Obes (Lond) **39:**1548–1557.
22. **Lumeng CN, Bodzin JL, Saltiel AR.** 2007. Obesity induces a phenotypic switch in adipose tissue macrophage polarization. J Clin Invest **117:**175–184.

23. **Mathis D.** 2013. Immunological goings-on in visceral adipose tissue. Cell Metab **17:**851–859.
24. **Min SY, Kady J, Nam M, Rojas-Rodriguez R, Berkenwald A, Kim JH, Noh HL, Kim JK, Cooper MP, Fitzgibbons T, Brehm MA, Corvera S.** 2016. Human 'brite/beige' adipocytes develop from capillary networks, and their implantation improves metabolic homeostasis in mice. Nat Med **22:**312–318.
25. **Molofsky AB, Nussbaum JC, Liang HE, Van Dyken SJ, Cheng LE, Mohapatra A, Chawla A, Locksley RM.** 2013. Innate lymphoid type 2 cells sustain visceral adipose tissue eosinophils and alternatively activated macrophages. J Exp Med **210:**535–549.
26. **Mombaerts P, Iacomini J, Johnson RS, Herrup K, Tonegawa S, Papaioannou VE.** 1992. RAG-1-deficient mice have no mature B and T lymphocytes. Cell **68:**869–877.
27. **Montgomery MK, Hallahan NL, Brown SH, Liu M, Mitchell TW, Cooney GJ, Turner N.** 2013. Mouse strain-dependent variation in obesity and glucose homeostasis in response to high-fat feeding. Diabetologia **56:**1129–1139.
28. **Muoio DM, Newgard CB.** 2006. Obesity-related derangements in metabolic regulation. Annu Rev Biochem **75:**367–401.
29. **Nicholls DG, Locke RM.** 1984. Thermogenic mechanisms in brown fat. Physiol Rev **64:**1–64.
30. **Nishimura S, Manabe I, Nagasaki M, Eto K, Yamashita H, Ohsugi M, Otsu M, Hara K, Ueki K, Sugiura S, Yoshimura K, Kadowaki T, Nagai R.** 2009. $CD8^+$ effector T cells contribute to macrophage recruitment and adipose tissue inflammation in obesity. Nat Med **15:**914–920.
31. **Pi-Sunyer X.** 2009. The medical risks of obesity. Postgrad Med **121:**21–33.
32. **Prendergast C, Gidding SS.** 2014. Cardiovascular risk in children and adolescents with type 2 diabetes mellitus. Curr Diab Rep **14:**454.
33. **Sellers RS, Clifford CB, Treuting PM, Brayton C.** 2011. Immunological variation between inbred laboratory mouse strains: points to consider in phenotyping genetically immunomodified mice. Vet Pathol **49:**32–43.
34. **Shabalina IG, Petrovic N, de Jong JM, Kalinovich AV, Cannon B, Nedergaard J.** 2013. UCP1 in brite–beige adipose tissue mitochondria is functionally thermogenic. Cell Reports **5:**1196–1203.
35. **Shultz LD, Ishikawa F, Greiner DL.** 2007. Humanized mice in translational biomedical research. Nat Rev Immunol **7:**118–130.
36. **Stefanovic-Racic M, Yang X, Turner MS, Mantell BS, Stolz DB, Sumpter TL, Sipula IJ, Dedousis N, Scott DK, Morel PA, Thomson AW, O'Doherty RM.** 2012. Dendritic cells promote macrophage infiltration and comprise a substantial proportion of obesity-associated increases in CD11c+ cells in adipose tissue and liver. Diabetes **61:**2330–2339.
37. **Talukdar S, Oh DY, Bandyopadhyay G, Li D, Xu J, McNelis J, Lu M, Li P, Yan Q, Zhu Y, Ofrecio J, Lin M, Brenner MB, Olefsky JM.** 2012. Neutrophils mediate insulin resistance in mice fed a high-fat diet through secreted elastase. Nat Med **18:**1407–1412.
38. **Waller-Evans H, Hue C, Fearnside J, Rothwell AR, Lockstone HE, Calderari S, Wilder SP, Cazier JB, Scott J, Gauguier D.** 2013. Nutrigenomics of high fat diet induced obesity in mice suggests relationships between susceptibility to fatty liver disease and the proteasome. PLoS One **8:**1–12.
39. **Weisberg SP, McCann D, Desai M, Rosenbaum M, Leibel RL, Ferrante AW Jr.** 2003. Obesity is associated with macrophage accumulation in adipose tissue. J Clin Invest **112:**1796–1808.
40. **West DB, Boozer CN, Moody DL, Atkinson RL.** 1992. Dietary obesity in 9 inbred mouse strains. Am J Physiol **262:**R1025–R1032.
41. **Winer S, Chan Y, Paltser G, Truong D, Tsui H, Bahrami J, Dorfman R, Wang Y, Zielenski J, Mastronardi F, Maezawa Y, Drucker DJ, Engleman E, Winer D, Dosch HM.** 2009. Normalization of obesity-associated insulin resistance through immunotherapy. Nat Med **15:**921–929.
42. **Wolf MJ, Adili A, Piotrowitz K, Abdullah Z, Boege Y, Stemmer K, Ringelhan M, Simonavicius N, Egger M, Wohlleber D, Lorentzen A, Einer C, Schulz S, Clavel T, Protzer U, Thiele C, Zischka H, Moch H, Tschop M, Tumanov AV, Haller D, Unger K, Karin M, Kopf M, Knolle P, Weber A, Heikenwalder M.** 2014. Metabolic activation of intrahepatic $CD8^+$ T cells and NKT cells causes nonalcoholic steatohepatitis, and liver cancer via cross-talk with hepatocytes. Cancer Cell **26:**549–564.
43. **Wu D, Molofsky AB, Liang HE, Ricardo-Gonzalez RR, Jouihan HA, Bando JK, Chawla A, Locksley RM.** 2011. Eosinophils sustain adipose alternatively activated macrophages associated with glucose homeostasis. Science **332:**243–247.
44. **Wu J, Bostrom P, Sparks LM, Ye L, Choi JH, Giang AH, Khandekar M, Virtanen KA, Nuutila P, Schaart G, Huang K, Tu H, van Marken Lichtenbelt WD, Hoeks J, Enerback S, Schrauwen P, Spiegelman BM.** 2012. Beige adipocytes are a distinct type of thermogenic fat cell in mouse and human. Cell **150:**366–376.
45. **Xu H, Barnes GT, Yang Q, Tan G, Yang D, Chou CJ, Sole J, Nichols A, Ross JS, Tartaglia LA, Chen H.** 2003. Chronic inflammation in fat plays a crucial role in the development of obesity-related insulin resistance. J Clin Invest **112:**1821–1830.